Theor Chem Acc (2010) 127:69–80
DOI 10.1007/s00214-009-0706-x

REGULAR ARTICLE

Mechanistic pathways for the reaction of quercetin with hydroperoxy radical

Zoran S. Marković · Jasmina M. Dimitrić Marković · Ćemal B. Doličanin

Received: 1 October 2009 / Accepted: 20 November 2009 / Published online: 4 December 2009

Abstract The extensive theoretical study of the interaction of one of the most abundant and reactive flavonols, quercetin, with hydroperoxy radical (HOO·), using the M052X/6-31 + Gd, p level of theory, was performed. Results indicating that quercetin is not a planar molecule are in accord with the X-ray analysis. The applied method successfully reproduces the bond dissociation enthalpy, and reveals that the reaction of quercetin with the hydroperoxy radical is governed by a hydrogen atom transfer mechanism. It is confirmed that the 3′OH and 4′OH are the most reactive sites, and that the reaction in the 3′OH position is faster than that in the 4′OH position.

Keywords Quercetin · DFT · M052X · Hydroperoxy radical

1 Introduction

Flavonoids are reported to exert a wide range of positive attributes like elimination of singlet oxygen, reduction of lipid peroxidation, termination of the propagation phase in which hydro-peroxy lipids are formed, detoxification of hydrogen peroxide through non-enzymatic defense mechanisms, diminishing the oxidative stress and many others [1–4].

Very often these in vitro-obtained results of extraordinary antioxidant activity of flavonoids are simply extrapolated to the conditions in vivo, which is not quite correct concerning the fact that their heath benefits go beyond regulating reactive radical species [5]. Their in vivo activity is largely dependent on several factors their bioavailability, heterogeneity of natural media, in vivo redox status, the degree of their degradation by gut microorganisms and factors related to their basic structure, including major determinants like their molecular size, the degree of glycosylation, the hydroxylation pattern, the presence of the C4 carbonyl group, double bond between C2 and C3 conjugated with the 4-oxo group, C3 hydroxyl group present in flavonols, the level of conjugation with other polyphenols and their interactions with surrounding molecules [1–7].

Oxygen radicals (superoxide anion O_2^-, hydroxyl-HO·; peroxy-ROO·; alkoxyl-RO· nitric oxide-NO·) are highly reactive oxidative species able to chemically react with a great number of organic compounds in biological and chemical systems. In the terms of the half-life, and consequently the reactivity, peroxy radical form is not the leading one but is very important in biological systems because it can pass readily through the cell membranes and cannot be excluded from them. It is actually necessary for the function of many enzymes, and thus is, like oxygen itself, required for good health to be maintained [8–10]. Under biological conditions, it is formed by the monovalent reduction of the superoxide.

There are two fundamental and widespread reaction pathways through which flavonoids (ArOH) and other phenolic compounds scavenge free radicals (1) rapid

Electronic supplementary material The online version of this article (doi:10.1007/s00214-009-0706-x) contains supplementary material, which is available to authorized users.

Z. S. Marković · Ć. B. Doličanin
Department of Bio-chemical and Medical Sciences, State University of Novi Pazar, Vuka Karadžića bb, 36300 Novi Pazar, Republic of Serbia

J. M. Dimitrić Marković (✉)
Faculty of Physical Chemistry, University of Belgrade, Studentski trg 12-16, 11000 Belgrade, Republic of Serbia
e-mail: markovich@ffh.bg.ac.rs

donation of the hydrogen atom to a radical form forming a new radical, more stable than the initial one (Hydrogen atom transfer [HAT] mechanism leading to the direct O–H bond breaking)

$$\mathrm{ArOH} + \mathrm{HO}\cdot \rightarrow \mathrm{ArO}\cdot + \mathrm{HOH} \quad (1)$$

and (2) the chain-breaking mechanism, by which the primary antioxidant transforms into radical cation by donating an electron to the free radical present in the system (e.g., lipid or some other radical). This mechanism is leading to indirect H-abstraction.

$$\mathrm{ArOH} + \mathrm{HO}\cdot \rightarrow \mathrm{ArOH}^{+} + \mathrm{OH}^{-} \rightarrow \mathrm{ArO}\cdot + \mathrm{HOH} \quad (2)$$

The net result of the reactions (1) and (2) is the same and both, H-atom transfer and electron transfer occur in parallel by different rates. Besides the HAT mechanism, where the proton and the electron are transferred together, many important biochemical processes, proceed via proton-coupled electron transfer (PCET) mechanism, which occurs when a proton and electron are transferred between different sets of molecular orbitals [11–14]. Both HAT and PCET mechanisms depend upon the medium investigated. In general they are governed by the strength of the phenolic O–H bond, i.e., by the O–H bond dissociation enthalpy (BDE), the molecular property used in the assessment of possible radical scavenging potential of the molecule. BDE is calculated as the difference in enthalpy between the molecule (quercetin in this case) and its radicals, implicating its correspondence to the OH bond breaking energy (the weaker the OH bond is, the smaller BDE is and the faster HAT mechanism will be leading to the faster reaction with free radical). The electron-transfer mechanism (Eq. 2) is governed by one-electron transfer process with both the ionization potential and reactivity of the radical-cation ArOH^{+} playing important role. Whatever mechanism is involved the formed radical specie ArO· needs to be relatively stable, so that reactions 1 and 2 could be thermodynamically favorable in the sense that it is easier to remove a hydrogen atom from ArOH than from HOH. In such a way antioxidant molecule will react slowly with the substrate and faster with the radical form preventing or postponing toxic effects (such is the oxidative stress) of its reaction with the substrate molecules. It is also important to emphasize that both, antioxidant molecule and the final product obtained from it, should be non-toxic and should not exert pro-oxidant effect [15].

Quercetin is naturally occurring and the most abundant dietary flavonol commonly found in onions and other vegetables and fruits. Because of its specific structural features, it is considered as a highly potent antioxidant capable of effective free radical scavenging under in vivo. This paper addresses the potential antioxidant activity of each of the quercetin reactive sites in simulated reactions with hydroperoxy free radical. The structure–activity relationship is examined in the light of the obtained results. For the investigation of the reaction of quercetin and hydroperoxy radical the M052X/6-31 + G** level of theory is used.

2 Computation methods

Geometry optimization, energies, and first and second energy derivatives of all stationary points are calculated using the new local density functional method (M05-2X) that is recently developed by the Truhlar group [16, 17]. This new hybrid meta exchange–correlation functional is parameterized so that it includes both nonmetallic and metallic compounds. Also, this functional yields satisfactory overall performance for the main group thermochemistry and thermochemical kinetics, as well as organic, organometallic, biological and noncovalent interactions [16–19]. The 6-31 + G(d,p) basis set [20] is used, as a quite large basis set for a molecular system of such size and as a unique and enough-tested set of basic functions for H-atom transfer reactions. The choice of this basis set is also motivated by the fact that it gives reliable BDE, estimation in the gas phase (enthalpy difference, calculated at 298 K, for the reaction ArOH → ArO· + H·) and better description of electronic interaction far from the nucleus (i.e., electron delocalization), due to the joint use of polarization functions (d,p) and diffuse functions (+). All ArO· radicals are evaluated by using an unrestricted scheme in order to take spin polarization into account, which is required in such density functional theory (DFT) calculations.

The vibrational frequencies are obtained from diagonalization of the corresponding M05-2X Hessian matrices. The nature of the stationary points is determined by analyzing the number of imaginary frequencies: 0 for minimum and 1 for transition state. Relative energies were calculated at 298 K. Zero point corrections (ZPE) and thermal corrections (TCE) to energy are included. The M05-2X/6-31 + G(d,p) values are corrected by using the recommended scaling factor 0.9631 [21]. All calculations were conducted using Gaussian03 [22].

3 Results and discussion

The notation used in this work follows as the molecule of quercetin (Scheme 1), its radical formed by H-removal from the 3-OH group and corresponding transition state are denoted with Q, 3-OH radical and TS3, respectively. The same notation is used for the other four radical forms and corresponding transition states.

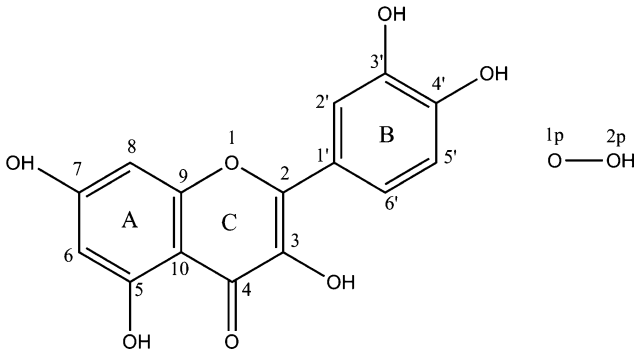

Scheme 1 Atomic numbering of quercetin and hydroperoxyl radical

3.1 Structure of quercetin

The results on conformational space of Q as a function of torsional angle τ (C3–C2–C1′–C2′) between the rings B and C and their preferred relative positions are presented in Fig. 1. By removing constrain for the torsional angle the conformational absolute minimum is found at $\tau = 169.6°$ (structure I in Fig. 1). A local minimum of very similar energy (higher by 0.16 kcal/mol) is found at $\tau = 12.0°$ (structure II in Fig. 1). The maximum of the potential energy lies at $\tau = 90°$ and the intercorvesion barrier between the two minima is about 5.9 kcal/mol. All hydroxyl groups are oriented in such way to form the maximum number (three) of hydrogen bonds.

The geometrical parameters of the absolute minimum for the structure I are reported in supplementary information together with all the parameters of the intermediates (radicals) and data coming from X-ray crystallographic measurements [23], which are compared to the calculated the geometrical parameters for Q. The percentage errors for bond lengths and bond angles between the calculated geometrical parameters of Q and its X-ray crystallographic data are 1.1 and 1.4%. The accuracy of the obtained results is similar to that of Leopoldini et al. [24] at the B3LYP/6-31 ++G** level of theory, and somewhat higher than that of Dhaouadi et al. [25] at the B3LYP/6-31 ++G* level of theory. Some OH bond lengths and bond angles have higher percentage errors. In particular, the errors for the O3–H3, O5–H5, and O7–H7 bond lengths, and C3–O3–H3, C5–O5–H5, and C4′–O4′–H4′ angles amount 7.5, 3.7, 5.2, 4.7, 6.2 and 8.9%, respectively. This means that the calculated OH bonds are overestimated. It is possible to suppose that all these differences may be due to the crystal packing in the lattice.

If the differences between the vacuum and condensed phase environments are taken into account it is possible to say that M05-2X/6-31 + G** level of theory reproduces geometrical parameters of Q quite well. It is also worth mentioning that in going from $\tau = 0°$ to $\pm 30°$, the potential energy curve is very flat with an energy variation of about 0.22 kcal/mol meaning that the planar conformation is easily obtained requiring a negligible amount of energy. This small deviation from the planarity of the molecule preludes a possible extended delocalization with a consequent good stabilization of the radical species eventually originating from the hydrogen abstraction from the OH groups in all the rings. As indicated by Rice–Evans et al. [26] and by van Acker et al. [27], the antioxidant properties of flavonoids can be derived just from their good delocalization possibilities.

Previous semiempirical [28, 29], ab initio [30] and DFT [24] studies suggest that the absolute minimum geometrical features are very similar to those obtained in the present investigation. The only exception is the value of the τ torsion angle which, at the AM1, RHF/6-31G* and B3LYP/6-311 ++G** levels, is found to be 153.3° [21], 162.3° and 180° [24]. The density functional M05-2X/6-31 + G** value (169.6°) is much closer to the experimental torsion angle of 172.1° [23]. Using the AM1 [28], RHF/6-31G* [29] and B3LYP/6-311 ++G** [24] methods, the energy difference between conformations of the two minima is estimated to be 0.23, 0.20, and 0.55 kcal/mol, respectively, and the rotation barrier required to pass from conformation I to II is 2.5, 5, and 5.59 kcal/mol. The M05-2X/6-31 + G** results are relatively close to these values. Although the sets of theoretical data are slightly different they underline univocally an easy rotation around the τ angle and a very small energy gap between the two stable conformations suggesting their probable coexistence (Fig. 2).

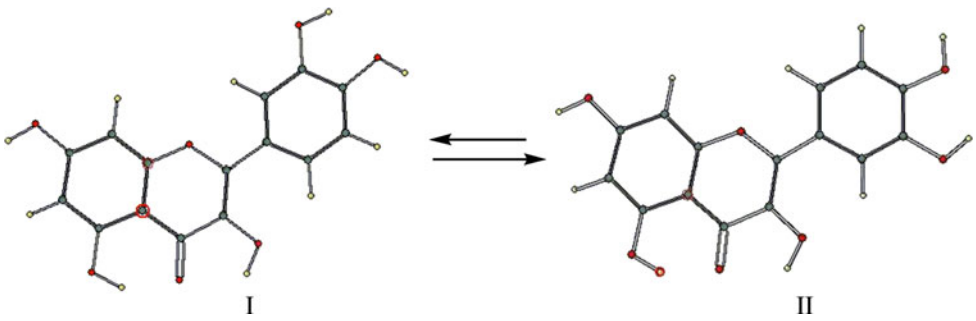

Fig. 1 Two most stable M052X/6-31G** optimized structures of quercetin molecule in the gas phase (I and II)

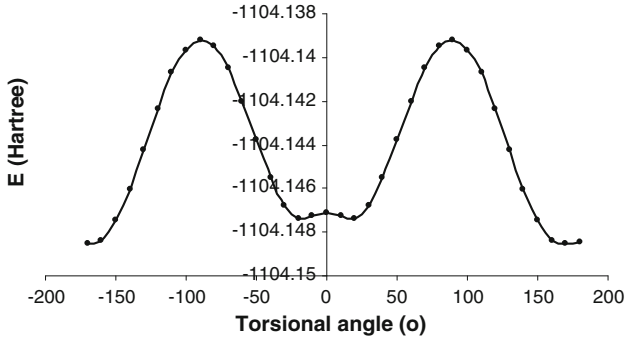

Fig. 2 Rotation barrier around the inter C2–C1′ bond calculated with the M052X/6-31 + G** method for the structure I

As the conformer I is more stable than the conformer II all further investigations address the conformer I.

3.2 BDE of quercetin

Among the five hydroxyl groups of Q, 3′OH and 4′OH groups in the B ring (catechol moiety) are the most responsible for the antioxidant activity [24, 31, 32]. As the calculated BDE values confirm [24, 25, 33] even 3OH group, in some cases, can be also responsible for antioxidant activity. Theoretical calculations of the BDE, using either semi-empirical Hartree–Fock method or DFT, have been useful for elucidating the high capacity of the OH groups of phenolic antioxidants [17, 18, 31–41]. Nevertheless, quantum-chemical studies on flavonoids are far from being complete. The most theoretical investigations are focused only on the B-ring (particularly the catechol moiety) and the most reliable methodology still has to be established.

The present study is focused on the reaction of HOO· radical and Q, in order to elucidate the reactivity of these OH groups and the corresponding radical forms formed after H-abstraction. Although the B3LYP method is used in many investigations on antioxidant activity in this study the M05-2X method is applied. The main reason lies in the fact that sometimes there are some problems in the prediction of bond dissociation energies, as well as energies and geometries of transition states using B3LYP method [42–44].

In order to check the quality of the applied M052X/6-31 + G** level of theory, the BDE values obtained by it are compared to the BDE data for Q available in literature. The gas-phase B3LYP/6-311 ++G** BDE value of Q, computed with reference to its most stable radical species, is 72.35 kcal/mol [24]. This value is smaller by 10.54 kcal/mol with respect to the phenol BDE value (82.89 kcal/mol), at the same theoretical level [28], indicating a better activity of Q as radical scavenger. The phenol experimental value for BDE of 86.7 ± 0.7 kcal/mol at 1 atm standard state is recommended by Murder et al. [45]. The B3LYP/6-311 + G** BDE of 87.10 kcal/mol [46] is nearer to the experimental value, and is obtained by a computational procedure in which the radical is treated using a restricted open-shell approach instead of an unrestricted one. Furthermore, an H-atom correction of 1.36 kcal/mol is also introduced [47]. The BDE values predicted with M052X/6-31 + G** (Table 1) are generally higher than Leopoldin's [24] and especially than Dhaouadi's [25] data, but are consistent with Nenadis's and Li's data [46, 48]. If the values of BDE in Table 1 are carefully examined, it can be concluded that all methods predict the same sequence of the reactivity of OH groups: 4′OH > 3′OH > 3OH > 7OH > 5OH, except in the case when the B3LYP/6-31 ++G* method is applied [25].

Table 1 Bond dissociation enthalpies of quercetin

	BDE (kcal/mol)				
	4′OH	3′OH	3OH	5OH	7OH
B3P86/6-311 + G** [32]	74.6	77.0	83.7	93.3	88.6
B3LYP/6-311 + G** [32]	71.1	73.6	79.7	94.7	84.4
B3LYP/6-311 ++G** [24]	72.3	75.0	79.2	94.5	86.1
ONIOM-G3B3 [48]	78.7	81.8	85.5	99.9	93.2
B3LYP/6-31 ++G* [25]	67.6	78.9	76.2	89.9	81.5
M052X/6-31 + G**	77.5	80.1	86.1	101.6	94.4

3.3 Reactions of quercetin with hydroperoxy radical

Bearing in mind the reactivity of OH groups of Q obtained on the basis of the BDE values, we take a step further in this work, and investigate the reactions of all OH groups of Q with hydroperoxy radical. Hydroperoxy radical is chosen because numerous natural peroxides are of the similar structure (ROO·) so the obtained results could demonstrate their general behavior. The calculations reveal that detachment of H atom by hydroperoxy radical can be performed with all five hydroxyl groups of Q. Each reaction proceeds via one transition state and one intermediate (corresponding radical form). The mechanism is presented in Fig. 3 values of total energies, enthalpies and free energies of all relevant species are given in Table 2. Figure 4 presents the optimized geometries of all transition states.

3.4 Mechanism

During the reaction of n-OH group (n = 3′, 4′, 3, 5, and 7) with hydroperoxy radical, partial detachment of Hn atom from On is observed in transition state. The distance

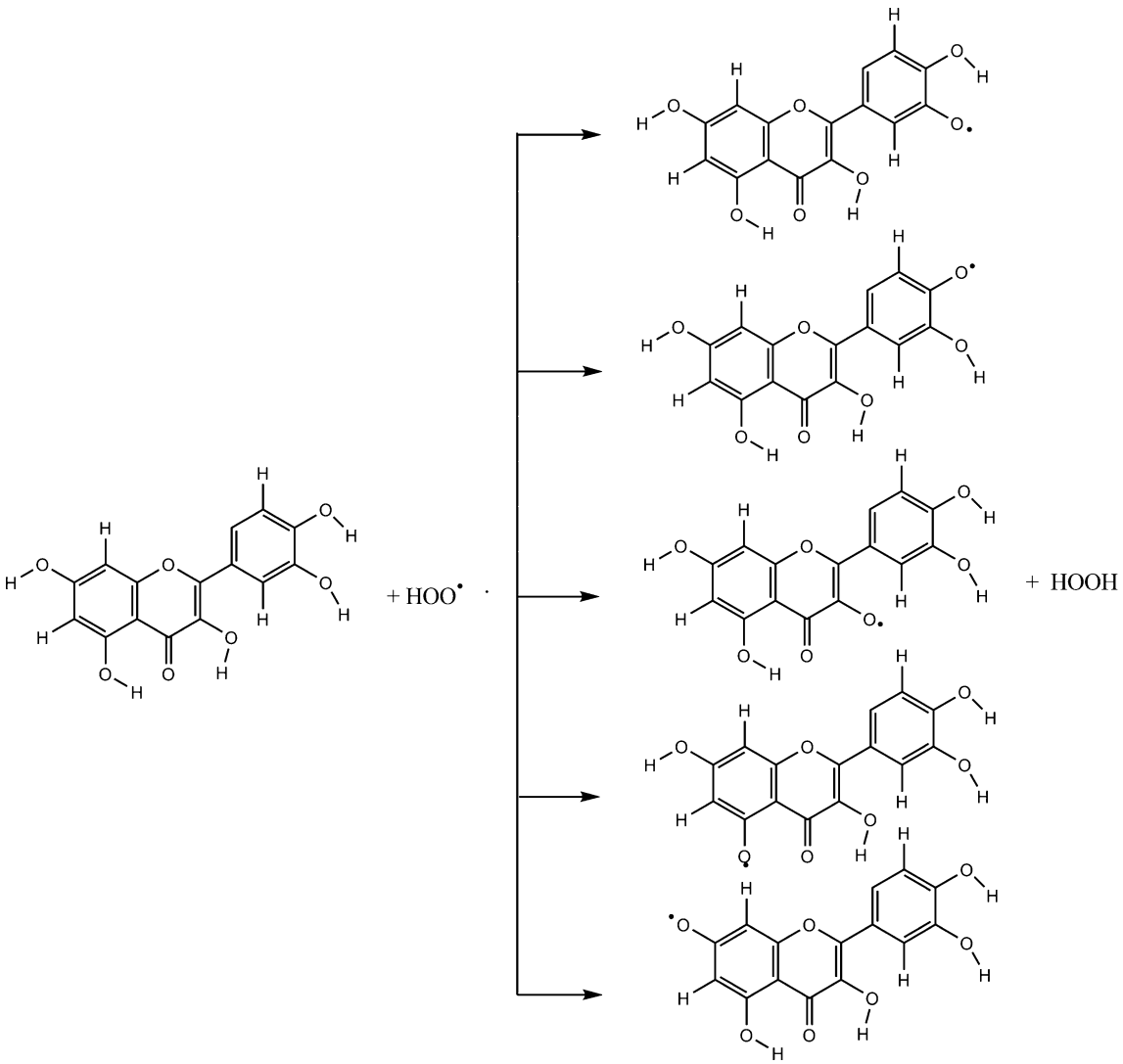

Fig. 3 Five reaction pathways for the reaction of quercetin with hydroperoxy radical

between On–Hn in TSn is increased with respect to corresponding bond in Q by 15.5, 15.9, 18.8, 33.1, and 23.3%, whereas the distance between Hn and O1p is longer than O–H bond in hydrogen peroxide (0.964 Å) by 32.7, 34.6, 25.8, 12.2, and 23.3% for $n = 3'$, $4'$, 3, 5, and 7, respectively. This indicates that TS3′ and TS4′ are early transition states, whereas TS5 is the late one.

A detailed analysis of the transition states charges shows that the QO and HOO fragments carry negative charge, while transferred H has a positive charge in all cases (see supporting information). In addition, spin density is also located on HOO and QO fragments. Actually, spin density associated with QO moiety is increased, while that associated with OOH fragment is decreased, in comparison to the reactants. However, there is no spin density associated with a transferred hydrogen atom. These facts indicate that reactions of quercetin OH groups with ·OOH radical proceed by HAT mechanism. Although the spin density on the transferred hydrogen can not be generally used to distinguish HAT from PCET mechanism [11] some other results also point to HAT mechanism: the analysis of the SOMOs shapes in transition states and the results of the optimized transition states with orientation of ·OOH moiety corresponding to PCET mechanism. The latter one shows that PCET is energetically unfavorable (for example, for Q3′ and Q4′ the activation energies are higher by 3.6 and 2.6 kcal/mol) comparing to HAT. This finding is in agreement with the experimental research of Musialik et al. [49] on the reactions of flavonoids with peroxyl and dpph radicals in non-polar solvent.

The selected orbital occupancies of Q, peroxy radical, and corresponding TSs are shown in Supplementary (Table 3). They are used to describe the nature of transfer in all

Table 2 Total energy (E), enthalpy (H^{298}), and free energy (G^{298}) for compounds under investigations

	E	H^{298}	G^{298}	Ratio
Q	–1,103.9226	–1,103.9080	–1,103.9702	
HOO	–150.8684	–150.8650	–150.8896	
HOOH	–151.4981	–151.4948	–151.5195	
4′OH	–1,103.3016	–1,103.2888	–1,254.8385	0.45
3′OH	–1,103.2982	–1,103.2846	–1,254.8392	1
3OH	–1,103.2894	–1,103.2751	–1,254.8317	3×10^{-4}
5OH	–1,103.2650	–1,103.2504	–1,254.8179	2×10^{-10}
7OH	–1,103.2765	–1,103.2618	–1,103.3244	3×10^{-7}
TS4′	–1,254.7861	–1,254.8385	–1,103.3474	
TS3′	–1,254.7862	–1,254.7690	–1,103.3440	
TS3	–1,254.7802	–1,254.7632	–1,103.3360	
TS5	–1,254.7648	–1,254.7473	–1,103.3474	
TS7	–1,254.7717	–1,254.7543	–1,103.3120	

Values of E, H^{298}, and G^{298} are scaled using appropriate scaling factors [14]. All values of energy are in Hartrees

reactions. From this table, it is clear that there is an unpaired electron in *p*-orbital on the Op1 oxygen atom in peroxy radical. This *p*-orbital overlaps with *s*-orbital of Hn atom from hydroxyl group of Q leading to a formation of the H-Op1 bond with occupancy close to 1.7. At the same time, On–Hn bond is breaking and the unpaired electron stays in the *p*-orbital of On. This causes overlapping between the *p*-orbitals of On and Cn and formation of the π-bonds with relatively high occupancies (about 1.7). In each TS*n*, anti-bonding orbitals (BD(2)*CnOn) and (BD(1)*HnOP1) are relatively highly occupied too meaning that the unpaired electron is mainly located in these orbitals.

The single occupied orbital (SOMO) of TS3′, TS4′, and TS3 (Fig. 5) shows that the unpaired electron is mainly delocalized among ring B, C3 atom of the ring C, and corresponding oxygen atoms (where deprotonation takes place). Figure 5 also reveals that delocalization of SOMO is significantly weaker in other two transition states (TS5 and TS7). These differences in delocalization of SOMOs can explain the higher activation energies for the reactions in the TS5 and TS7 positions.

The activation energy, ΔG, associated with each of these reactions is calculated as the difference in the total free energy between the transition state and corresponding reactant. The following energy activation sequence for the OH groups is found: 3′OH < 4′OH < 3OH < 7OH < 5OH (Table 2). By the Curtin-Hammond principle, the distribution of the products is determined according to the difference in free energies of the transition states. For this reason, the free energy differences between all transition states are calculated. The resulting ratios between the concentrations of the products are given in Table 2. On the basis of activation energies and distribution of the products it is obvious that the reactivity of the B-ring is higher than that of the C-ring and particularly A-ring. This is consistent with what is known from literature concerning structure–activity relationships of antioxidant flavonoids [26].

3.5 Reactions in positions O3′ and O4′

By inspecting Table 2, one can observe that the smallest activation energy of 12.92 kcal/mol is required for the reaction in the position 3′OH, while the reaction in the position 4′OH has slightly higher activation energy of 13.39 kcal/mol. This leads to a conclusion that the reaction can take place in both positions with similar probabilities. The reverse reactions in these positions are unlikely, since both reactions are exothermic.

The scavenging of the H3′ and H4′ atoms by the hydroperoxyl radical creates a perturbation that is more pronounced in the B ring, where strong variation of all bonds has been observed (see Fig. 4 and supporting information). The NBO analysis shows that there are double bonds between C2′–C3′, C4′–C5′ and C6′–C1′ in the B-ring of Q. In the TS3′, the double bonds are located between C1′–C2′, C5′–C6′ and C3′–O3′, and in the TS4′ between C1′–C2′, C5′–C6′ and C4′–O4′. Bond angles are almost equal as in Q, while dihedral angles between the rings C and B are slightly smaller ($\tau = 8.8°$ and 9.3° for TS3′ and TS4′, respectively).

After hydrogen abstraction has been completed, corresponding transition states grow into products, namely HOOH and either 3′OH or 4′OH radical forms. The 3′OH and 4′OH radical forms are characterized by three hydrogen bonds (Fig. 6) that contribute to the stabilization of each specie. Each radical form is additionally stabilized with relatively strong hydrogen bond between oxygen atom (where H-removal is performed) and hydrogen from neighboring OH group.

The NBO analysis allows further comment on the electronic structure of the obtained radical isomers. The complete delocalization involves only ring A in both radicals, while the ring C is characterized by three double bonds strongly localized on the carbonyl group, C2–C3 and C9–C10 bonds. Significant difference in comparison to the parent molecule of Q is the existence of strongly localized double bonds on the carbonyl group at C4′, as well as between the C2′–C3′ and C5′–C6′ atoms in 4′OH radical. In the case of 3′OH radical form, the localized double bonds are located on the carbonyl group at C3′, between the C1′–C2′ and C5′–C6′ atoms.

Within an unrestricted scheme, the spin density is often considered to be a more realistic parameter providing a better representation of the stability. The importance of the

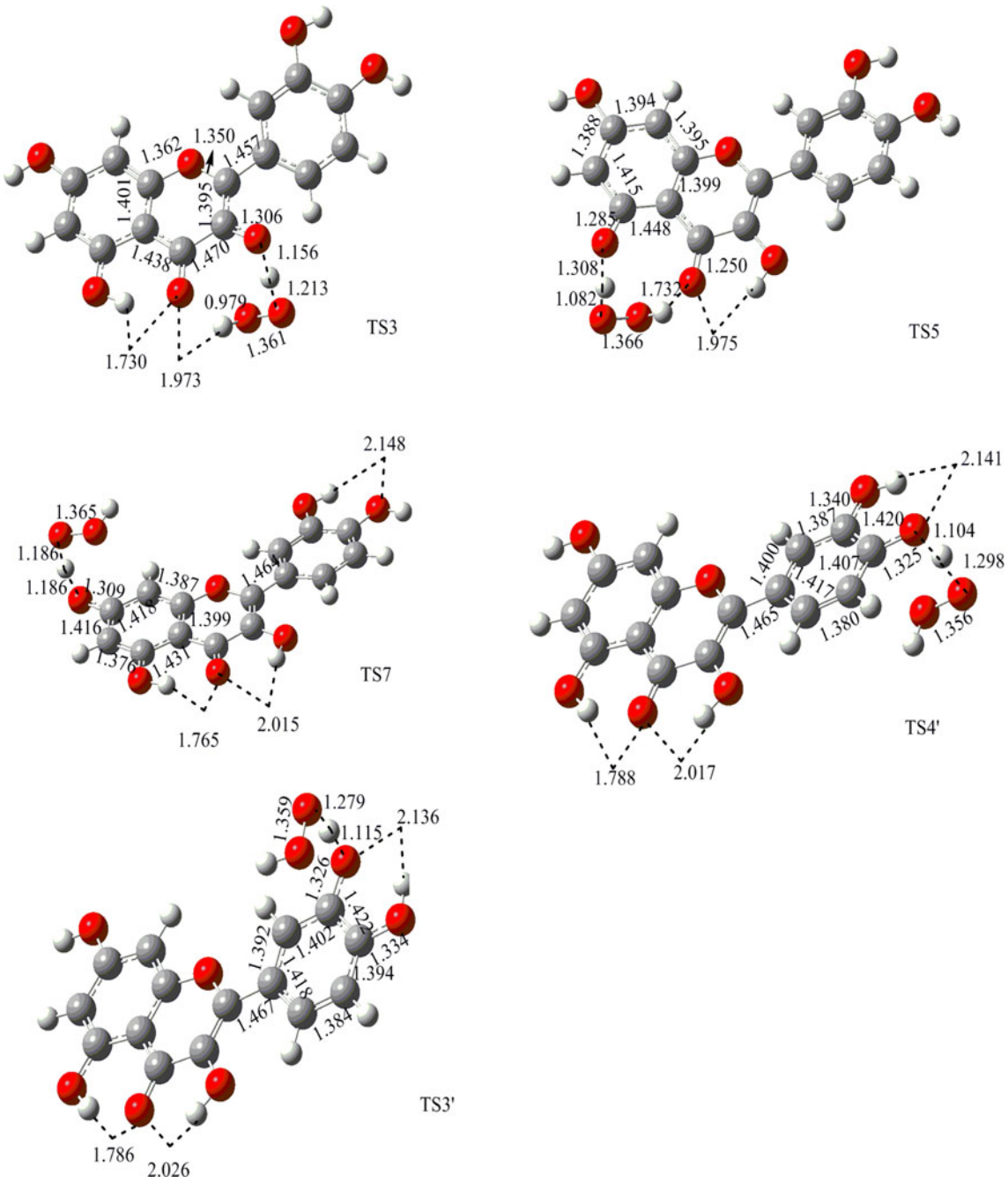

Fig. 4 The geometries of transition states

spin density for the description of flavonoids has been pointed out by the recent papers of Leopoldini et al. [24, 32] and Trouillas et al. [33]. In this paper, the spin density on the QO radical forms is also analysed, in order to understand the differences in their stabilities.

The spin density appears to be slightly more delocalized for radicals issued from the B-ring (4′OH and 3′OH) than for that located on the A-ring (5OH and 7OH) (Fig. 6). This is a consequence of the presence of the C2–C3 double bond, which allows for spin presence on the C3 atom (0.18 for 4′-OH). The spin distribution indicates the oxygen O atom bonded to C4′ as the most probable radical center, followed by the carbon atom C1′.

This effect can be explained by using the classical resonance effects occurring in the phenoxy radical. Such a scheme explains the presence of the radical (high spin density) on the C1′ atom in para-position for the 4′-OH radical specie, and the subsequent possible delocalization effect due to the presence of the C2–C3 double bond. It is to be noted that such delocalization cannot happen in 3′OH

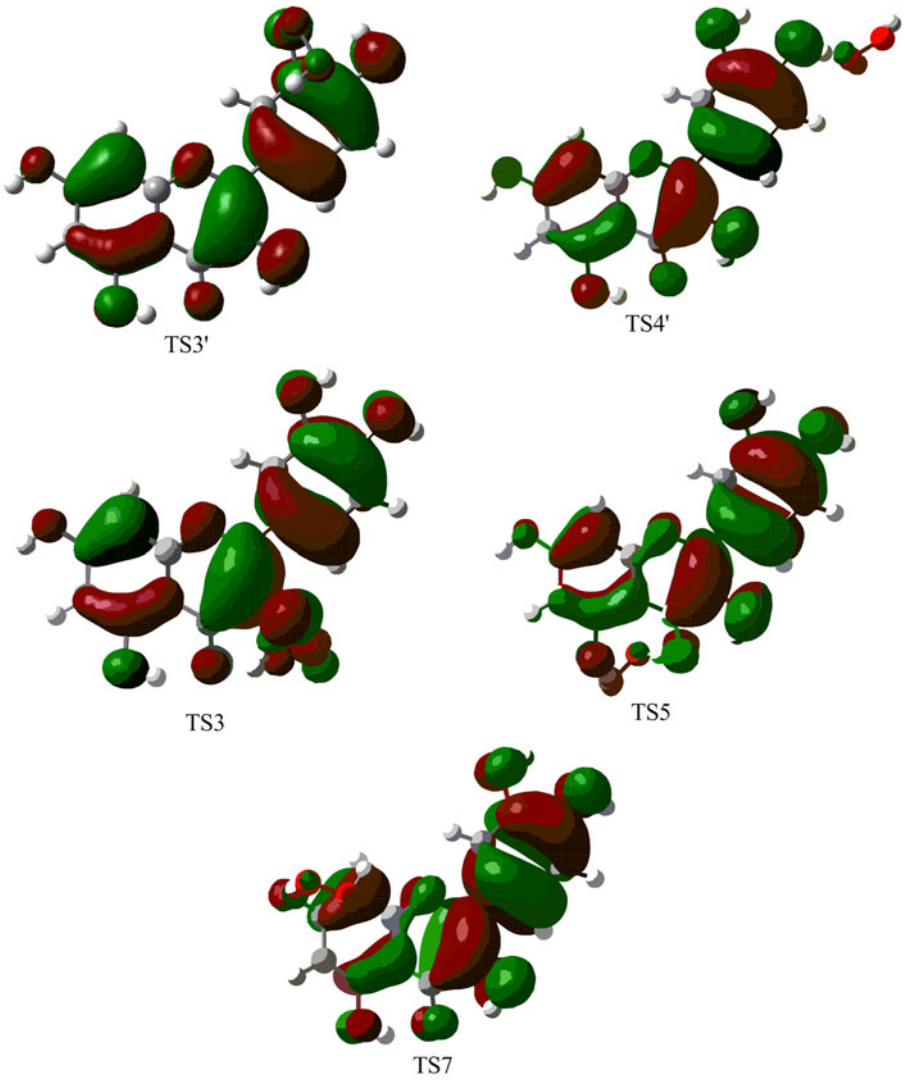

Fig. 5 The shape of SOMO in different transition states

radical form due to high spin densities on the C6′ and C4′. Stronger delocalization in 4′OH radical specie is confirmed by hybrid composition of respective bonds. It is found that slightly greater *s*-orbital contribution in hybrid composition for the C2–C1′ bond ($sp^{1.67}$–$sp^{2.17}$) in 4′OH radical form, comparing to the corresponding bond in Q ($sp^{1.71}$–$sp^{2.27}$), offers stronger electron delocalization over the ring C than in Q. On the other hand, for 3′OH radical form, a similar hybrid composition is found for the C2–C1′ bond ($sp^{1.73}$–$sp^{2.23}$) as for corresponding bond in Q. We suppose that this stronger electron delocalization in the case of 4′OH radical specie is the main reason why this radical is more stable than the 3′OH one. It is worth pointing out that the intraconversion of gained radicals is also possible to happen where relatively small activation energy is needed for the H transfer process (6.3 kcal/mol for the transfer from 3′OH to 4′OH form and 8.5 kcal/mol for the reverse process). This means that even though 3′OH radical form is obtained in excess amounts, it can easily be transformed into more stable 4′OH radical form.

3.6 Reaction in position O3

Beside the most reactive sites 3′OH and 4′OH the 3OH position is also interesting for reaction with hydroperoxy radical. The activation barrier for a formation of TS3 is by 4.7 and 4.3 kcal/mol higher than those for TS3′ and TS4′ implying that H-transfer from the 3OH group is also possible, depending on the oxidative system. This assumption is based on several in vitro studies confirming the participation of the 3-OH group in redox reactions [50, 51]. In addition, reverse reaction in this position is plausible, since the reaction is endothermic.

In TS3 hydrogen of OOH· radical forms week hydrogen bond with nearby carbonyl group. The abstraction of the H3 atom by the radical creates a perturbation, which is

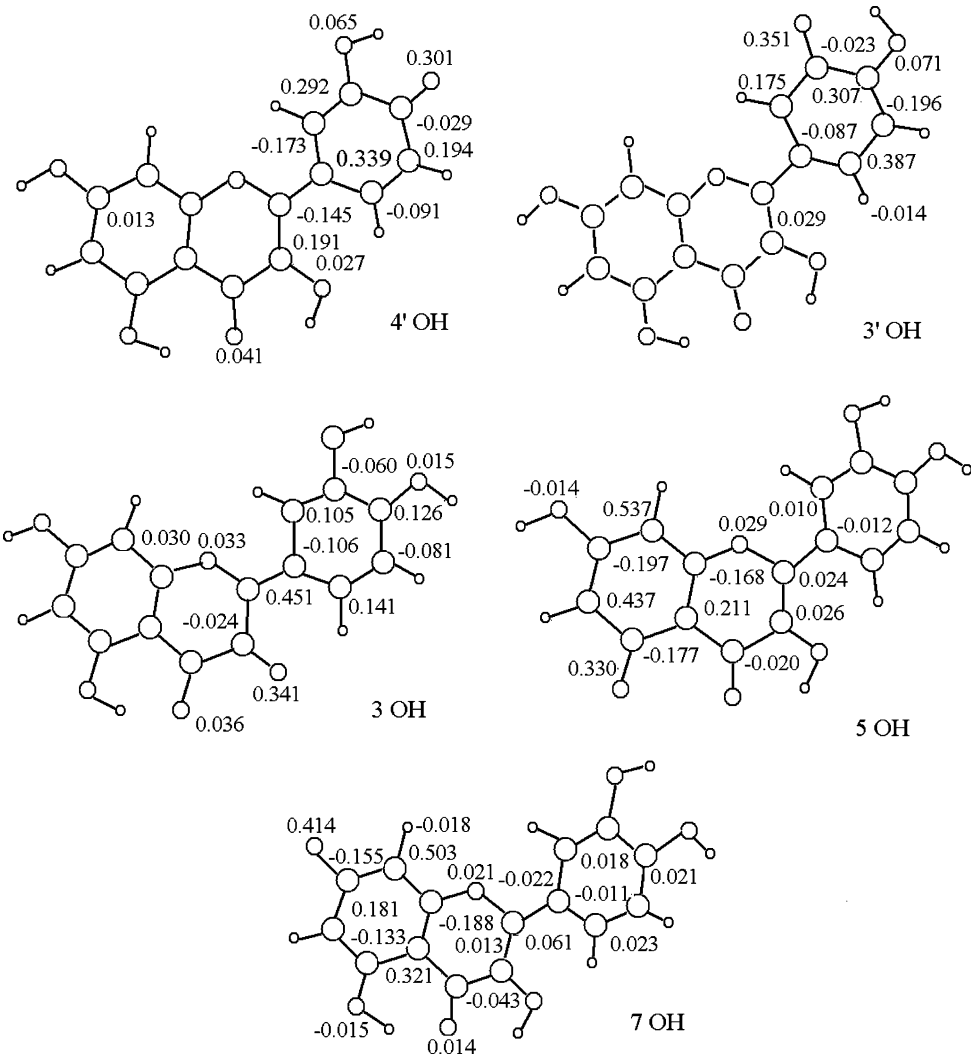

Fig. 6 Distribution of spin densities in the radicals formed by H-removal from Q

more pronounced in the C ring, where strong variation of the C3–O3, C2–C3, C3–C4 and O1–C2 bonds is observed, comparing to Q (see Fig. 3 and supporting information). In addition, complete rearrangement of double bonds in rings A and C is found in transition state. The double bonds are now located between C5–C6, C8–C9, C3–O3 and C4–O4. The NBO analysis is in accordance with this finding, since it reveals that only the ring B is delocalized in TS3. Bond angles are almost equal to those in Q, while dihedral angle between the rings C and B is significantly increased ($\tau = 19.5°$). Based on this value, one can suppose that electron delocalization between the rings B and C is significantly hindered and that this hindrance is an important reason for higher activation energy comparing to activation energy required for the reaction performed on the 3′OH and 4′OH groups.

As a product of this reaction, the 3OH radical is formed. The investigation reveals that the geometry of the 3OH radical form is significantly different from that of Q. All bond lengths are more or less changed, and this particularly refers to the O1–C2, C3–O3, C4–O4 and C3–C4 bonds. Concerning bond angles, all values are very similar to those of Q, except in the cases of C2–C3–O4 and C6–C7–O7. It is worth pointing out that the dihedral angle between the rings B and C becomes planar. Thus, complete delocalization involves only rings A and B, while the ring C is characterized by two double bonds strongly localized on the carbonyl groups. Due to the planarity around the torsional angle τ the electronic flow between the ortho-diphenolic moiety and the ring C is still possible. This conclusion is supported by hybrid composition and the C2–C1′ bond length. Slightly smaller *p*-orbital contribution ($sp^{1.62}$–$sp^{2.15}$), comparing to the corresponding bond in Q, offers better electron delocalization over the B ring.

Our investigation shows that, though there is weak spin delocalization over the ring B, spin density is mainly located on the O3 and C2 atoms. This finding indicates the carbon C2 as the most probable radical center (Fig. 6), followed by the oxygen atom bonded to carbon C3. This result is in agreement with that of Trouillas et al. [33]. It is

well known that keto–enol tautomerism can take place in Q and since the quercetin keto form is markedly less stable than the enol one (by about 20 kcal/mol), the contribution of the keto form can be considered negligible for quercetin as a free molecule. For this reason, the possible mechanism for H-abstraction from the C2 atom is not considered in this paper.

3.7 Reactions in positions O5 and O7

Though the reactions of the hydroperoxy radical with Q in the positions 5OH and 7OH are unlikely, the main characteristics of their transition states and radicals are also presented in the text that follows. The activation energies for TS5 and TS7 are higher than those for TS3′ by 13.3 and 8.9 kcal/mol, respectively, and both reactions are endothermic. The activation barriers for reverse reactions in the C5 and C7 positions are 8.5 and 11.8 kcal/mol implying that reverse reactions are plausible (Fig. 1; Table 2).

The NBO analysis reveals that only the ring B is delocalized in TS5 and TS7. Strong variation of the bond lengths and complete rearrangement of double bonds in the ring A relative to Q are found. As confirmed with the NBO analysis and bond lengths, the double bonds in TS5 are located between C5–O5, C6–C7 and C9–C10, and between C7–O7, C5–C6 and C9–C10 in TS7. In TS5, hydrogen of the hydroperoxy radical forms strong hydrogen bond (1.732 Å) with carbonyl group in the position C4. When the reaction occurs in the position C7 there is no similar stabilization of the transition state by the hydrogen bond. It may be the reason for higher energy of TS7.

The NBO analysis of the products of these reactions reveals that rings A and B are characterized by five double bonds strongly localized on the carbonyl groups of both radicals, between C6–C7, C2–C3, and C9–C10 bonds in the 5OH radical, and between C2–C3, C5–C6, and C9–C10 bonds in the 7OH radical. Since the C2–C1′ bond length is the same in both radical forms, while hybrid compositions are very similar to those in Q, it can be expected that electronic flow between the ortho-diphenolic moiety and the ring C are also similar to that in Q. On the other hand, electronic flow between the ortho-diphenolic moiety and the ring A is prevented in both cases, because there is no conjugation between the rings A and C.

The results of this investigation demonstrate that there is practically no spin delocalization over the rings B and C in both radicals. The spin density is mainly located on the C8, C6 and O5 atoms of the 5OH radical form (Fig. 6). This result indicates the carbon C8 as the most probable radical center, followed with C6. On the other hand, spin density analysis for the 7OH radical indicates the carbon C8 as the most probable radical center, followed with O7 (Fig. 6). Our finding slightly differs from that of Trouillas et al. [33] who proposed that spin density was almost equally distributed among the C8, C6 and O5 atoms in the 5OH radical, and between the C8 and O7 atoms in the 7OH radical.

4 Conclusion

The geometry of quercetin (Q) is investigated using the M052X/6-31 + Gd, p level of theory. This method turned out to be quite reliable for description of the properties of Q. In agreement with the X-ray crystallographic data, and with some previous theoretical results, it was found that Q is not planar molecule. The BDE values, obtained by this level of theory, are in agreement with the same values of other theoretical researches. The analysis of the natural bond orbital charges and orbital occupancies, as well as the SOMOs of the reactants, transition states and products shows that the reaction of Q with the hydroperoxy radical is governed by HAT mechanism. The most reactive sites are 3′OH and 4′OH, and the reaction in the 3′OH position is faster than the reaction in the 4′OH position. This result slightly disagrees from the BDE results, since the 4′OH radical form has lower BDE value. Furthermore, intramolecular hydrogen rearrangement from 3′OH to 4′OH radical form, with relatively small activation energy, is found.

To obtain more clarified picture of this mechanism, the solvent effects need to be taken into account. The investigation of the influence of different solvents upon the mechanism of the reaction is under intense scrutiny.

Acknowledgments The authors acknowledge financial support by the Ministry of Science and Environmental of Republic of Serbia (Grant No. 142025). Authors would like to thank all the Referees, especially to the anonymous Referee 2, for the detailed and critical reading of our manuscript.

References

1. Cody V, Middleton E, Harborne JB (1986) Plant flavonoids in biology and medicine: biochemical, pharmacological and structure-activity relationships. Alan R. Liss, New York
2. Cody V, Middleton EJR, Harborne JB, Beretz A (1988) Plant flavonoids in biology and medicine II: biochemical, cellular and medicinal properties. Alan R. Liss, New York
3. Rice-Evans C, Miller N (1996) Antioxidant activities of flavonoids as bioactive components of food. Biochem Soc Trans 24:790–794
4. Harborne JB, Williams CA (2000) Advances in flavonoid research since 1992. Phytochemisty 55:481–504
5. Shen L, Ji HF, Zhang HY (2007) How to understand the dichotomy of antioxidants. Biochem Biophys Res Commun 362:543–545
6. Cao G, Sofic E, Prior R (1997) Antioxidant and prooxidant behavior of flavonoids: structure- activity relationships. Free Radical Biol Med 22(5):749–760

7. Bravo L, Abia R, Eastwood MA, Saura-Calixto F (1994) Degradation of polyphenols (catechin and tannic acid) in the rat intestinal tract. Effect on coloic fermentation and faecal output. Br J Nutr 71:933–946
8. Pryor WA (ed) (1976) Free radicals in biology, vol I. Academic Press, New York
9. Pryor WA (1986) Oxy-radicals and related species: their formation, lifetimes, and reactions. Ann Rev Physiol 48:657–667
10. Fridovich I (1978) The biology of oxygen radicals. Science 20:875–880
11. Mayer JM (2004) Proton-coupled electron transfer: a reaction chemist's view. Annu Rev Phys Chem 55:363–390
12. DiLabio GA, Johnson ER (2007) Lone pair-π and π–π interactions play an important role in proton-coupled electron transfer reactions. J Am Chem Soc 129:6199–6203
13. DiLabio GA, Ingold KU (2005) A theoretical study of the iminoxyl/oxime self-exchange reaction. A five-center, cyclic proton-coupled electron transfer. J Am Chem Soc 127:6693–6699
14. Sjodin M, Styring S, Åkermark B, Sun L, Hammarstrom L (2000) Proton-coupled electron transfer from tyrosine in a tyrosine—ruthenium—tris-bipyridine complex: comparison with tyrosine$_z$ oxidation in photosystem II. J Am Chem Soc 122:3932–3936
15. Mulder P, Korth HG, Ingold KU (2005) Why quantum–thermochemical calculations must be used with caution to indicate "a promising lead antioxidant". Helvetica Chimica Acta 88:370–374
16. Zhao Y, Truhlar DG (2008) The M06 suite of density functionals for main group thermochemistry, thermochemical kinetics, noncovalent interactions, excited states, and transition elements: two new functionals and systematic testing of four M06-class functionals and 12 other functionals. Theor Chem Acc 120:215–241
17. Zhao Y, Schultz NE, Truhlar DG (2005) Exchange-correlation functional with broad accuracy for metallic and nonmetallic compounds, kinetics, and noncovalent interactions. J Chem Phys 123:161103(1–5)
18. Zhao Y, Schultz NE, Truhlar DG (2006) Design of density functionals by combining the method of constraint satisfaction with parametrization for thermochemistry, thermochemical kinetics, and noncovalent interactions. J Chem Theory Comput 2(2):364–382
19. Zhao Y, Truhlar DG (2006) A new local density functional for main-group thermochemistry, transition metal bonding, thermochemical kinetics, and noncovalent interactions. J Chem Phys 125:194101(1–18)
20. Here WJ, Radom L, Schleyer PVR, Pople JA (1986) Ab initio molecular orbital theory. Wiley, New York
21. Merrick JP, Moran D, Radom L (2007) An evaluation of harmonic vibrational frequency scale factors. J Phys Chem 111:11683–11700
22. Frisch MJ, Trucks GW, Schlegel HB, Scuseria GE, Robb MA, Cheeseman JR, Zakrzewski VG, Montgomery JA Jr, Stratmann RE, Burant JC, Dapprich S, Millam JM, Daniels AD, Kudin KN, Strain MC, Farkas O, Tomasi J, Barone V, Cossi M, Cammi R, Mennucci B, Pomelli C, Adamo C, Clifford S, Ochterski J, Petersson GA, Ayala PY, Cui Q, Morokuma K, Malick AD, Rabuck KD, Raghavachari K, Foresman JB, Cioslowski J, Ortiz JV, Baboul AG, Stefanov BB, Liu G, Liashenko A, Piskorz P, Komaromi I, Gomperts R, Martin RL, Fox DJ, Keith T, Al-Laham MA, Peng CY, Nanayakkara A, Challacombe M, Gill PMW, Johnson B, Chen W, Wong MW, Andres JL, Gonzalez C, Head-Gordon M, Replogle ES, Pople JA (2003) Gaussian 03, ReVision E.01-SMP. Gaussian Inc., Pittsburgh
23. Jin GZ, Yamagata Y, Tomita KI (1990) Structure of quercetin dihydrate. Acta Cryst 46(2):310–313
24. Leopoldini M, Marino T, Russo N, Toscano M (2004) Density functional computations of the energetic and spectroscopic parameters of quercetin and its radicals in the gas phase and in solvent. Theor Chem Acc 111:210–216
25. Dhaouadi Z, Nsangou M, Garrab N, Anouar EH, Marakchi K, Lahmar S (2009) DFT study of the reaction of quercetin with O_2 and OH radicals. J Mol Struct THEOCHEM. doi:10.1016/j.theochem.2009.02.034
26. Rice-Evans CA, Miller NJ, Paganga G (1996) Structure-antioxidant activity relationships of flavonoids and phenolic acids. Free Radic Biol Med 20:933–938
27. van Acker SABE, van den Berg DJ, Tromp MNJL, Griffen DH, van Bennekom WP, van Der Vijgh WJ, Bast A (1996) Structural aspects of antioxidant activity of flavonoids. Free Radic Biol Med 20:331–338
28. Russo N, Toscano M, Uccella N (2000) A theoretical study of the conformational behavior and electronic structure of taxifolin correlated with the free radical-scavenging activity. J Agric Food Chem 48:3232–3240
29. Vasilescu D, Girma R (2002) Quantum molecular modeling of quercetin—simulation of the interaction with the free radical t-BuOO. Int J Quantum Chem 90:888–902
30. van Acker SABE, de Groot MJ, van den Berg DJ, Tromp MNJL, Donne′-Op den Kelder GM, Wim JF, van Der Vijgh WJF, Bast A (1996) A quantum chemical explanation of the antioxidant activity of flavonoids. Chem Res Toxicol 9:1305–1312
31. Leopoldini M, Marino T, Russo N, Toscano M (2004) Antioxidant properties of phenolic compounds: H-atom versus electron transfer mechanism. J Phys Chem A 108:4916–4923
32. Leopoldini M, Pitarch IP, Russo N, Toscano M (2004) Structure, conformation, and electronic properties of apigenin, luteolin, and taxifolin antioxidants. A first principle theoretical study. J Phys Chem A 108:92–96
33. Trouillas P, Marsal P, Siri D, Lazzaroni R, Duroux JL (2006) A DFT study of the reactivity of OH groups in quercetin and taxifolin antioxidants: the specificity of the 3-OH site. Food Chem 97:679–688
34. Lemaska K, Szymusiak H, Tyrakowska B, Zieliski R, Soffers AEMF, Rietjens IMCM (2001) The influence of pH on antioxidant properties and the mechanism of antioxidant action of hydroxyflavones. Free Rad Biol Med 31:869–881
35. Lucarini M, Pedulli GF, Guerra M (2004) A critical evaluation of the factors determining the effect of intramolecular hydrogen bonding on the O-H bond dissociation enthalpy of catechol and of flavonoid antioxidants. Chem Eur J 10:933–939
36. Priyadarsini KI, Maity DK, Naik GH, Kumar MS, Unnikrishnan MK, Satav JG (2003) Role of phenolic O-H and methylene hydrogen on the free radical reactions and antioxidant activity of curcumin. Free Radic Biol Med 35:475–484
37. Trouillas P, Fagne're C, Lazzaroni R, Calliste CA, Marfak A, Duroux JL (2004) A theoretical study of the conformational behavior and electronic structure of taxifolin correlated with the free radical-scavenging activity. Food Chem 88:571–582
38. Wright JS, Johnson ER, DiLabio GA (2001) Predicting the activity of phenolic antioxidants: theoretical method, analysis of substituent effects, and application to major families of antioxidants. J Am Chem Soc 123:1173–1183
39. Zhang HY, Sun YM, Chen DZ (2001) O–H bond dissociation energies of phenolic compounds are determined by field/inductive effect or resonance effect. A DFT study and its implication. QSAR 20:148–152
40. Zhang HY, Sun YM, Wang XL (2003) Substituent effects on O–H bond dissociation enthalpies and ionization potentials of catechols: a DFT study and its implications in the rational design of phenolic antioxidants and elucidation of structure-activity relationships for flavonoid antioxidants. Chem Eur J 9:502–508
41. Zhang HY (2004) On the effectiveness of the EPR radical equilibration technique in estimating O–H bond dissociation

enthalpies of catechols and other complex polyphenols. New J Chem 28:1284–1285
42. Check CE, Gilbert TM (2005) Progressive systematic underestimation of reaction energies by the B3LYP model as the number of C–C bonds increases: why organic chemists should use multiple DFT models for calculations involving polycarbon hydrocarbons. J Org Chem 70:9828–9834
43. Redfern PC, Zapol P, Curtiss LA, Raghavachari K (2000) Assessment of Gaussian-3 and density functional theories for enthalpies of formation of C1–C16 alkanes. J Phys Chem A 104:5850–5854
44. Grimme S (2006) Seemingly simple stereoelectronic effects in alkane isomers and the implications for Kohn-Sham density functional theory. Angew Chem Int Ed 45:4460–4464
45. Mulder P, Horth HG, Pratt DA, DiLabio GA, Valgimigli L, Pediulli GF, Ingold KU (2005) Critical re-evaluation of the O–H bond dissociation enthalpy in phenol. J Phys Chem A 109:2647–2655
46. Menadis N, Wang LF, Tsimidou MZ, Zhang HY (2005) Radical scavenging potential of phenolic compounds encountered in *O. europaea* products as indicated by calculation of bond dissociation enthalpy and ionization potential values. J Agric Food Chem 53:295–303
47. DiLabio GA, Pratt DA, LoFaro AD, Wright JS (1999) Theoretical study of X–H bond energetics (X = C, N, O, S): application to substituent effects, gas phase acidities, and redox potentials. J Phys Chem A 103:1653–1661
48. Li MJ, Liu L, Fu Y, Guo QX (2007) Accurate bond dissociation enthalpies of popular antioxidants predicted by the ONIOM-G3B3 method. J Mol Struct THEOCHEM 815:1–9
49. Musialik M, Kuzmicz R, Pawłowski TS, Litwinienko G (2009) Acidity of hydroxyl groups: an overlooked influence on antiradical properties of flavonoids. J Org Chem 74:2699–2709
50. Balogh-Hergovich E, Kaiser J, Speier G (1997) Synthesis and characterization of copper(I) and copper (II) flavonolate complexes with phthalazine ligand, and their oxygenation and relevance to quercetinase. Inorg Chim Acta 256:9–14
51. Marfak A, Trouillas P, Allais DP, Calliste CA, Duroux JL (2004) Reactivity of flavonoids with 1-hydroxyethyl radical: a γ-radiolysis study. Biochem Biophys Acta Gen Subjects 1670:28–39